
Posterior Variance Analysis of Gaussian Processes with Application to Average Learning Curves

Armin Lederer

Technical University of Munich
armin.lederer@tum.de

Jonas Umlauf

Technical University of Munich
jonas.umlauft@tum.de

Sandra Hirche

Technical University of Munich
hirche@tum.de

Abstract

The posterior variance of Gaussian processes is a valuable measure of the learning error which is exploited in various applications such as safe reinforcement learning and control design. However, suitable analysis of the posterior variance which captures its behavior for finite and infinite number of training data is missing. This paper derives a novel bound for the posterior variance function which requires only local information because it depends only on the number of training samples in the proximity of a considered test point. Furthermore, we prove sufficient conditions which ensure the convergence of the posterior variance to zero. Finally, we demonstrate that the extension of our bound to an average learning bound outperforms existing approaches.

1 Introduction

Gaussian process (GP) regression is a probabilistic supervised machine learning method that bases on Bayesian principles [1]. GP regression generalizes efficiently with little training data, which makes it appealing to real world applications with limited amount of training data. Therefore, it has gained increasing attention in the field of reinforcement learning and system identification for control design in recent years. Especially, when safety guarantees are necessary, GPs are the method of choice in active and reinforcement learning [2, 3, 4, 5] as well as control [6, 7, 8, 9, 10, 11]. These safety critical applications have in common that they rely on the posterior variance for deriving uniform error bounds [12, 13]. However, the behavior of the posterior variance when data points are added on-line, e.g. during control tasks, has barely been analyzed formally due to a lack of suitable bounds. Therefore, there is generally little understanding of the interaction between learning and control in feedback systems, which is crucial to provide guarantees for the control error.

Considering uniform training data distributions, the average posterior variance of GPs has extensively been studied, see [14, 15, 16, 17]. The mapping between this average variance and the number of training samples is usually referred to as *average learning curve* and it is used to evaluate the generalization properties of GPs. Although average learning curves have been applied to few applications, e.g., [18], they provide important theoretical insights to the learning behavior of GPs [19, 20]. This understanding can be exploited in sparse GP approximations in a similar way as proposed for PAC-Bayesian error bounds in [21]. Furthermore, active learning and experiment design can be an application scenario of average learning curves since common criteria such as the mutual information [22] also measure the generalization error. However, the framework developed for average learning curves is directly applicable to continuous input spaces, while it is difficult to evaluate the mutual information in this setting.

The contribution of this paper is a novel bound for the posterior variance of GPs with Lipschitz continuous covariance kernels. and demonstrate and improvement of the bound for a more specific class of kernels. Furthermore, we derive sufficient conditions for the generation of training data which ensure the convergence of our posterior variance bounds to zero and investigate criteria for probability distributions such that the convergence conditions are satisfied. Finally, we show a straight forward extension of our bounds to average learning curve bounds and compare our results to numerically obtained approximations. In fact, our average learning curve bound can be seen as generalization of the approach in [23], which our method outperforms.

The remaining paper is structured as follows: In Section 2, we provide an overview of related work on posterior variance bounds and average learning curves. Novel posterior variance bounds and necessary conditions on their convergence are derived in Section 3. Finally, the derived bounds are compared to approximations in Section 4.

2 Related Work

2.1 Gaussian Process Regression

A Gaussian process is a stochastic process such that any finite number of outputs¹ $\{y_1, \dots, y_M\} \subset \mathbb{R}$ is assigned a joint Gaussian distribution with prior mean 0 and covariance defined through the kernel $k : \mathbb{R}^d \times \mathbb{R}^d \rightarrow \mathbb{R}$ [1]. Therefore, the training outputs $y^{(i)}$ can be considered as observations of a sample function $f : \mathbb{X} \subset \mathbb{R}^d \rightarrow \mathbb{R}$ of the GP distribution perturbed by i.i.d. zero mean Gaussian noise with variance σ_n^2 . Regression is performed by conditioning the prior GP distribution on the training data $\mathbb{D}_N = \{(\mathbf{x}^{(i)}, y^{(i)})\}_{i=1}^N$ and a test point \mathbf{x} . The conditional posterior distribution is again Gaussian and can be calculated analytically. For this reason, we define the kernel matrix \mathbf{K}_N and the kernel vector $\mathbf{k}_N(\mathbf{x})$ through $K_{N,ij} = k(\mathbf{x}^{(i)}, \mathbf{x}^{(j)})$ and $k_{N,i}(\mathbf{x}) = k(\mathbf{x}, \mathbf{x}^{(i)})$, respectively, with $i, j = 1, \dots, N$. Then, the posterior mean $\mu_N(\cdot)$ and variance $\sigma_N^2(\cdot)$ are given by

$$\mu_N(\mathbf{x}) = \mathbf{k}_N^T(\mathbf{x})\mathbf{A}_N^{-1}\mathbf{y}_N, \quad (1)$$

$$\sigma_N^2(\mathbf{x}) = k(\mathbf{x}, \mathbf{x}) - \mathbf{k}_N^T(\mathbf{x})\mathbf{A}_N^{-1}\mathbf{k}_N(\mathbf{x}), \quad (2)$$

where $\mathbf{A}_N = \mathbf{K}_N + \sigma_n^2\mathbf{I}_N$ denotes the data covariance matrix and $\mathbf{y}_N = [y^{(1)} \dots y^{(N)}]^T$.

2.2 Posterior Variance Bounds and Average Learning Curve Bounds

A common measure to analyze the learning speed of GPs are average learning curves, which are also called integrated mean squared errors [17]. Under the assumption that $y^{(i)}$ are noisy observations of a function $f(\cdot)$, which is a sample function from the GP, the mean squared error of the posterior GP is given by $E_y[(y - \mu_N(\mathbf{x}))^2] = \sigma_N^2(\mathbf{x}) + \sigma_n^2$. The average learning curve is obtained from this equation by taking the expectation with respect to the test point \mathbf{x} and the input training data $\mathbb{D}_N^x = \{\mathbf{x}^{(i)}\}_{i=1}^N$, i.e., $e(N) = E_{\mathbb{D}_N^x}[E_x[\sigma_N^2(\mathbf{x}) + \sigma_n^2]]$. For notational simplicity of the following derivations, we consider the uniform distributions over the unit interval $\mathbb{X} = [0, 1]$ in the following. However, all derivations can be extended to higher dimensional state spaces and other distributions even though it is a little technical.

A simple approach to obtain a learning curve bound for GPs with isotropic kernels, which only depend on the distance between their arguments $k(x, x') = k(\|x - x'\|)$, proposed in [23] bases on the idea to consider only the training samples $x^{(i)}$ closest to x in the variance calculation. This approach leads to a valid posterior variance bound since the posterior variance cannot increase by adding training samples [24]. Considering only the nearest training sample in the calculation of the posterior variance (2) directly leads to

$$\sigma_N^2(x) \leq \sigma_1^2(x) = k(0) - \frac{k^2(\tau)}{k(0) + \sigma_n^2}, \quad (3)$$

¹Vectors/matrices are denoted by lower/upper case bold symbols, the $n \times n$ identity matrix by \mathbf{I}_n , the Euclidean norm by $\|\cdot\|$, sets by upper case black board bold letters. Sets restricted to positive numbers have an indexed $+$, e.g. \mathbb{R}_+ for all positive real valued numbers. The cardinality of sets is denoted by $|\cdot|$. The expectation operator $E[\cdot]$ can have an additional index to specify the considered random variable. Class \mathcal{O} notation is used to provide asymptotic upper bounds on functions. The ceil and floor operator are denoted by $\lceil \cdot \rceil$ and $\lfloor \cdot \rfloor$, respectively.

with τ being the minimal Euclidean distance between x and the training data set \mathbb{D}_N^x , i.e. $\tau = \min_{x' \in \mathbb{D}_N^x} \|x - x'\|$. Assume that the training data is ordered by increasing value of x and divide the unit interval in N segments such that the boundaries are given by $a_1 = 0$, $a_i = (x^{(i)} + x^{(i-1)})/2$, $b_{i-1} = (x^{(i)} + x^{(i-1)})/2$, $b_N = 1$ for $i = 2, \dots, N$. Then, the expectation with respect to the test points can be approximated by $E_x[\sigma_N^2(x)] \leq \sum_{i=1}^N \int_{a_i}^{b_i} \sigma_1^2(\xi) d\xi$. Exploiting (3) and symmetry of the covariance, it is straightforward to show that these integrals only depend on the distance δ between training samples. Therefore, the expectation with respect to the training data \mathbb{D}_N^x reduces to an expectation with respect to δ , such that the average learning curve can be bounded by

$$e(N) \leq \bar{e}_1(N) = k(0) + \sigma_n^2 - 2 \frac{E_\delta \left[\int_0^\delta k^2(\tau) d\tau \right]}{k(0) + \sigma_n^2} - 2(N-1) \frac{E_\delta \left[\int_0^{\frac{\delta}{2}} k^2(\tau) d\tau \right]}{k(0) + \sigma_n^2}. \quad (4)$$

The expectations in this bound can be calculated analytically for some kernels since the difference δ between adjacent points follows first order statistics, hence, we have $p(\delta) = N(1 - \delta)^{N-1}$. However, they are typically computed numerically [23].

When considering the two closest training samples, the inverse in (2) still leads to a simple expression which leads to the following posterior variance bound

$$\sigma_N^2(x) \leq \sigma_2^2(x) = k(0) - \frac{k(0) + \sigma_n^2(k^2(\tau_2) + k^2(\tau_1)) - 2k(\eta)k(\tau_1)k(\tau_2)}{(k(0) + \sigma_n^2)^2 - k^2(\eta)}, \quad (5)$$

where τ_1 and τ_2 are the distances to the two closest training samples and δ is the distance between the two closest training samples. By defining segments with $a_1 = 0$, $a_i = x^{(i-1)}$, $b_{i-1} = x^{(i-1)}$, $b_{N+1} = 1$ for $i = 2, \dots, N+1$, (5) and symmetry of the kernel can be exploited to derive an expression for the expectation with respect to the test points which depends only on the distance δ between training points, such that we obtain the average learning curve bound

$$\bar{e}_2(N) = k(0) + \sigma_n^2 - 2(N-1) E_\delta \left[\frac{\int_0^\delta (k(0) + \sigma_n^2) k^2(\tau) + k(\delta) k(\tau) k(\delta - \tau) d\tau}{(k(0) + \sigma_n^2)^2 - k^2(\delta)} \right] - 2 \frac{E_\delta \left[\int_0^\delta k^2(\tau) d\tau \right]}{k(0) + \sigma_n^2}. \quad (6)$$

Although both bounds are relatively tight for small numbers of training data, they do not converge to the asymptotic value of the average learning curve σ_n^2 . Instead, the bound $\bar{e}_1(N)$ has been shown to converge to $\sigma_n^2(2 + \sigma_n^2)/(1 + \sigma_n^2)$, while $\bar{e}_2(N)$ converges to $\sigma_n^2(3 + \sigma_n^2)/(2 + \sigma_n^2)$ [23]. Therefore, these bounds do not provide any insight when analyzing the learning behavior with large data sets.

2.3 Literature Review

Some posterior variance bounds for GP regression have been developed as intermediate results in the context of Bayesian optimization, e.g., [25]. However, in this area, isotropic kernels are typically used which hinders the application outside of this field. For noise-free interpolation, the posterior variance has been analyzed using spectral methods [26]. While the asymptotic behavior can be analyzed efficiently with such methods, they are not suited to bound the posterior variance for specific training data sets. In the context of noise-free interpolation, many bounds from the area of scattered data approximation can be applied due to the equivalence of the posterior variance and the power function [27]. Therefore, classical results [28, 29, 30] as well as newer findings [31, 32] can be directly used for GP interpolation. However, it is typically not clear how these results can be generalized to regression with noisy observations.

For the derivation of average learning curves, many different approaches have been pursued in literature. A common method to approximate learning curves builds on spectral methods, e.g., [14, 15, 16, 33, 17]. This approach has also been extended to special situations such as learning on graphs [34] and multi-task learning [35, 36]. However, these approaches cannot be employed in any formal proof on the generalization properties of GPs since they only describe the approximate learning behavior. Therefore, some work has focused on deriving strict upper and lower bounds for average learning curves [37, 23]. However, the upper bounds in [23] suffer from the disadvantage, that they can only capture the learning behavior for few training samples. Hence, upper bounds for average learning curves are missing that are capable of describing the learning behavior for small as well as large data sets.

3 Posterior Variance of Gaussian Processes

Despite a wide variety of literature on average learning curves and posterior variance bounds for isotropic kernels, learning curve bounds and general posterior variance bounds have gained far less attention. Exploiting ideas from existing posterior variance bounds, we derive in Section 3.1 an upper bound on the posterior variance, which depends on the number of samples in the neighborhood of the test point \mathbf{x} . In Section 3.2 we derive sufficient conditions on probability distributions of the training data that ensure the convergence of our bound. Finally, we demonstrate how the derived bound for isotropic kernels can be applied to average learning curve bounds of GP in Section 3.3.

3.1 Posterior Variance Bound and Asymptotic Behavior

The central idea in deriving an upper bound for the posterior variance of a GP lies in the observation that data close to a test point \mathbf{x} usually lead to the highest decrease in the posterior variance. Therefore, it is natural to consider only training data close to the test point in the bound as more and more data is acquired. The following theorem formalizes this idea. The proofs for all the following theoretical results can be found in the supplementary material.

Theorem 3.1. *Consider a GP with Lipschitz continuous kernel $k(\cdot, \cdot)$ with Lipschitz constant L_k , an input training data set $\mathbb{D}_N^x = \{\mathbf{x}^{(i)}\}_{i=1}^N$ and observation noise variance σ_n^2 . Let $\mathbb{B}_\rho(\mathbf{x}) = \{\mathbf{x}' \in \mathbb{D}_N^x : \|\mathbf{x}' - \mathbf{x}\| \leq \rho\}$ denote the training data set restricted to a ball around \mathbf{x} with radius ρ . Then, for each $\mathbf{x} \in \mathbb{X}$ and $\rho \leq k(\mathbf{x}, \mathbf{x})/L_k$, the posterior variance is bounded by*

$$\sigma_N^2(\mathbf{x}) \leq \frac{(4L_k\rho - L_k^2\rho^2) |\mathbb{B}_\rho(\mathbf{x})| k(\mathbf{x}, \mathbf{x}) + \sigma_n^2 k(\mathbf{x}, \mathbf{x})}{|\mathbb{B}_\rho(\mathbf{x})| (k(\mathbf{x}, \mathbf{x}) + 2L_k\rho) + \sigma_n^2}. \quad (7)$$

The parameter ρ can be interpreted as information radius, which defines how far away from a test point \mathbf{x} training data is considered to be informative. However, this information radius is conservative as all the data points with smaller radius are treated in the theorem as if they had a distance of ρ to the test point. Therefore, a large ρ has the advantage that many training points are considered, while a small ρ is beneficial if sufficiently many training samples are close to the test point \mathbf{x} .

Note, that Theorem 3.1 is very general as it is merely restricted to Lipschitz continuous kernels, which is a common property of kernels for regression [1]. This generality comes at the price of tightness of the bound and tighter bounds exist under additional assumptions, e.g., the bound in [25] for isotropic, decreasing kernels, which have non-positive derivatives $\frac{\partial}{\partial \tau} k(\tau) \leq 0, \tau \geq 0$. However, this bound can directly be derived from Theorem 3.1, which leads to the following corollary.

Corollary 3.1. *Consider a GP with isotropic, decreasing covariance kernel $k(\cdot, \cdot)$, an input training data set $\mathbb{D}_N^x = \{\mathbf{x}^{(i)}\}_{i=1}^N$ and observation noise variance σ_n^2 . Let $\mathbb{B}_\rho(\mathbf{x}) = \{\mathbf{x}' \in \mathbb{D}_N^x : \|\mathbf{x}' - \mathbf{x}\| \leq \rho\}$ denote the training data set restricted to a ball around \mathbf{x} with radius ρ . Then, for each $\mathbf{x} \in \mathbb{X}$, the posterior variance is bounded by*

$$\sigma_N^2(\mathbf{x}) \leq k(0) - \frac{k^2(\rho)}{k(0) + \frac{\sigma_n^2}{|\mathbb{B}_\rho(\mathbf{x})|}}. \quad (8)$$

In addition, Theorem 3.1 can also be used for an asymptotic analysis of the posterior variance, i.e., $\lim_{N \rightarrow \infty} \sigma_N^2(\mathbf{x})$. Even though the limit of infinitely many training data cannot be reached in practice, this analysis is important because it helps to determine the amount of training data which is necessary to achieve a desired posterior variance. In the following corollary, we provide necessary conditions that ensure the convergence to zero of the bound (7).

Corollary 3.2. *Consider a GP with Lipschitz continuous kernel $k(\cdot, \cdot)$, an infinitely large input training data set $\mathbb{D}_\infty^x = \{\mathbf{x}^{(i)}\}_{i=1}^\infty$ and the observation noise variance σ_n^2 . Let $\mathbb{D}_N^x = \{\mathbf{x}^{(i)}\}_{i=1}^N$ denote the subset of the first N input training samples and let L_k be the Lipschitz constant of kernel $k(\cdot, \cdot)$. Furthermore, let $\mathbb{B}_\rho(\mathbf{x}) = \{\mathbf{x}' \in \mathbb{D}_N^x : \|\mathbf{x}' - \mathbf{x}\| \leq \rho\}$ denote the training data set restricted to a ball around \mathbf{x} with radius ρ . If there exists a function $\rho : \mathbb{N} \rightarrow \mathbb{R}_+$ such that*

$$\rho(N) \leq \frac{k(\mathbf{x}, \mathbf{x})}{L_k} \quad \forall N \in \mathbb{N} \quad (9)$$

$$\lim_{N \rightarrow \infty} \rho(N) = 0 \quad (10)$$

$$\lim_{N \rightarrow \infty} |\mathbb{B}_{\rho(N)}(\mathbf{x})| = \infty \quad (11)$$

holds, the posterior variance at \mathbf{x} converges to zero, i.e. $\lim_{N \rightarrow \infty} \sigma_N(\mathbf{x}) = 0$.

Although it might be unintuitive that the number of training samples in a ball with vanishing radius has to reach infinity in the limit of infinite training data, this is not a restrictive condition. Deterministic sampling strategies can satisfy it, e.g. if a constant fraction of the samples lies on the considered point \mathbf{x} or if the maximally allowed distance of new samples reduces with the total number of samples. Furthermore, this condition is satisfied for a wide class of probability distributions for sufficiently slowly vanishing radius $\rho(N)$ as shown in the following section.

Remark 3.1. *Corollary 3.2 does not require dense sampling in a neighborhood of the test point \mathbf{x} . In fact, the conditions on the training samples in Corollary 3.2 are satisfied if the data is sampled densely, e.g., from a manifold which contains the test point \mathbf{x} , such as a line through \mathbf{x} .*

3.2 Conditions on Probability Distributions for Asymptotic Convergence

For fixed ρ it is well known that the number of training samples inside the ball $\mathbb{B}_\rho(\mathbf{x})$ converges to its expectation due to the strong law of large numbers. Therefore, it is sufficient to analyze the asymptotic behavior of the expected number of samples inside the ball instead of the actual number for fixed ρ . However, it is not clear how fast the radius $\rho(N)$ is allowed to decrease in order to ensure convergence of $|\mathbb{B}_{\rho(N)}(\mathbf{x})|$ to its expected value. The following theorem shows that the admissible order of $\rho(N)$ depends on the local behavior of the density $p(\cdot)$ around \mathbf{x} .

Theorem 3.2. *Consider a sequence of points $\mathbb{D}_\infty^x = \{\mathbf{x}^{(i)}\}_{i=1}^\infty$ which is generated by drawing from a probability distribution with density $p(\cdot)$. If there exists a non-increasing function $\rho : \mathbb{N} \rightarrow \mathbb{R}_+$ and constants $c, \epsilon \in \mathbb{R}_+$ such that*

$$\lim_{N \rightarrow \infty} \rho(N) = 0 \tag{12}$$

$$\int_{\{\mathbf{x}' \in \mathbb{X} : \|\mathbf{x} - \mathbf{x}'\| \leq \rho(N)\}} p(\mathbf{x}') d\mathbf{x}' \geq cN^{-1+\epsilon}, \tag{13}$$

then, the sequence $|\mathbb{B}_{\rho(N)}(\mathbf{x})|$ goes to infinity almost surely, i.e. $\lim_{N \rightarrow \infty} |\mathbb{B}_{\rho(N)}(\mathbf{x})| = \infty$ a.s.

Similarly to Theorem 3.1, Theorem 3.2 is formulated very general to be applicable to a wide variety of probability distributions. However, under additional assumptions condition (36) can be simplified. This is exemplary shown for probability densities which are positive in a neighborhood of the considered point \mathbf{x} .

Corollary 3.3. *Consider a sequence of points $\mathbb{D}_\infty^x = \{\mathbf{x}^{(i)}\}_{i=1}^\infty$ which is generated by drawing from a probability distribution with density $p(\cdot)$, such that $p(\cdot)$ is positive in a ball around \mathbf{x} with any radius $\xi \in \mathbb{R}_+$, i.e.*

$$p(\mathbf{x}') > 0 \quad \forall \mathbf{x}' \in \{\mathbf{x}' : \|\mathbf{x} - \mathbf{x}'\| \leq \xi\}. \tag{14}$$

Then, for all non-increasing functions $\rho : \mathbb{N} \rightarrow \mathbb{R}_+$ for which exist $c, \epsilon \in \mathbb{R}_+$ such that

$$\rho(N) \geq cN^{-\frac{1}{d}+\epsilon} \quad \forall N \in \mathbb{N} \tag{15}$$

$$\lim_{N \rightarrow \infty} \rho(N) = 0 \tag{16}$$

it holds that $\lim_{N \rightarrow \infty} |\mathbb{B}_{\rho(N)}(\mathbf{x})| = \infty$ a.s.

This corollary shows that it is relatively simple to allow the maximum decay rate of $\rho(N) \approx N^{-1}$ for scalar inputs. For higher dimensions d however, it cannot be achieved and the allowed decay rate decreases exponentially with d . Yet, this is merely a consequence of the curse of dimensionality.

3.3 Application to Average Learning Curves

Both posterior variance bounds in [23] suffer from the fact that they do not converge to zero in the limit of infinite training data. However, the idea used in [23] to derive (3) and (5) is the same as in Theorem 3.1. In fact, (3) can be seen as a special case of our bound in Corollary 3.1 with $|\mathbb{B}_\rho(\mathbf{x})| = 1$. Therefore, it is natural to employ (8) for the derivation of average learning curve bounds by choosing ρ such that $|\mathbb{B}_\rho(\mathbf{x})| = n > 1$. Furthermore, we divide the unit interval in $m =$

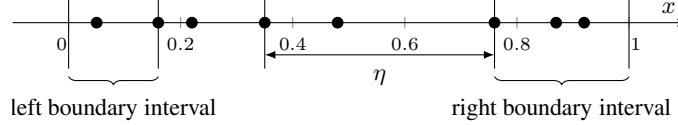


Figure 1: Fixed training data set with $N = 8$ and division such that inner intervals have $n = 3$ samples, left boundary interval $n_l = 2$ samples and right boundary interval $n_r = 3$ samples

$\lceil (N - 2n + 1)/(n - 1) \rceil$ inner sections and two boundary sections as depicted in Fig. 1 for $N = 8$ and $n = 3$. The inner sections are chosen such that each of them starts and ends at a training sample and contains exactly $n > 1$ of them. The remaining $N - m(n - 1) + 1$ training points are divided fairly among the two boundaries: the left boundary section contains $n_l = \lfloor (N - m(n - 1) + 1)/2 \rfloor$ and the right boundary section contains $n_r = \lceil (N - m(n - 1) + 1)/2 \rceil$ training samples such that they stop and start at training samples, respectively. Hence, we can bound the average learning curve by

$$\bar{e}_\rho(N) = k(0) + \sigma_n^2 - 2m \int_0^1 \frac{I_n(\delta)}{k(0) + \frac{\sigma_n^2}{n}} d\delta - 2 \int_0^1 \frac{I_{n_l+1}(\delta)}{k(0) + \frac{\sigma_n^2}{n_l}} d\delta - 2 \int_0^1 \frac{I_{n_r+1}(\delta)}{k(0) + \frac{\sigma_n^2}{n_r}} d\delta, \quad (17)$$

$$\text{where } I_n(\delta) = \binom{N}{n-1} (1-\delta)^{N-n-1} \delta^{n-2} \int_{\frac{\delta}{2}}^{\delta} k^2(\rho) d\rho, \quad (18)$$

due to the fact that the distance between n training samples follows order statistics. Note that the integral in (18) has the lower boundary $\frac{\delta}{2}$ since this is the minimal distance to either boundary. Therefore, the maximal distance to a training point inside the considered section varies between $\frac{\delta}{2}$ and δ . Due to Corollary 3.3, (8) converges to zero for uniformly sampled training data with a suitably defined $\rho(N)$. Hence, (17) must also converge to zero for this information radius $\rho(N)$ and is therefore capable of describing the learning behavior for both small and large training data sets.

4 Numerical Evaluation

In this section we illustrate the behavior of the proposed bounds. Section 4.1 compares our variance bounds to the exact posterior variance for uniformly sampled training data and training data sampled from a distribution which vanishes at the considered point. In Section 4.2 we demonstrate the derived bounds on average learning curves for isotropic kernels and compare them to existing approaches.

4.1 Posterior Variance Bounds

We compare the bounds in Theorem 3.1 and Corollary 3.1 to the exact posterior variance for GPs with a squared exponential, a Matérn kernel with $\nu = \frac{1}{2}$, a polynomial kernel with $p = 3$ and a neural network kernel. The posterior variance is evaluated at the point $x = 1$ for a uniform training data distribution $\mathcal{U}([0.5, 1.5])$. Furthermore, the length scale of the kernels is set to $l = 1$ where applicable and the noise variance is set to $\sigma_n^2 = 0.1$. In order to obtain a good value for the information radius ρ , consider the following approximation of (8) for isotropic kernels

$$\hat{\sigma}_\rho^2(1) \approx k(0) - \frac{k^2(\rho)}{k(0)} + \frac{k(0)\sigma_n^2}{N\rho k(0) + \sigma_n^2}, \quad (19)$$

where we use the expectation of $E[|\mathbb{B}_\rho(1)|] = N\rho$ instead of the random variable $|\mathbb{B}_\rho(1)|$. For the squared exponential kernel the Taylor expansion around $\rho = 0$ yields

$$k(0) - \frac{k^2(\rho)}{k(0)} \approx 2\frac{\rho^2}{l^2} + \mathcal{O}(\rho^3). \quad (20)$$

Therefore, for large N the best asymptotic behavior of (8) is achieved with $\rho(N) = cN^{-\frac{1}{3}}$ for the squared exponential kernel under uniform sampling and leads to $\hat{\sigma}_\rho^2(1) \approx \mathcal{O}(N^{-\frac{2}{3}})$. The same approach can be used to calculate the information radius $\rho(N)$ with the best asymptotic behavior of the bound in Corollary 3.1 for the Matérn kernel with $\nu = \frac{1}{2}$. This leads to $\rho(N) = cN^{-\frac{1}{2}}$ and an asymptotic behavior of $\hat{\sigma}_\rho^2(1) \approx \mathcal{O}(N^{-\frac{1}{2}})$. For the non-isotropic kernels, we pursue a similar approach and substitute the expected number of samples $N\rho$ in (7), which results in the asymptotically

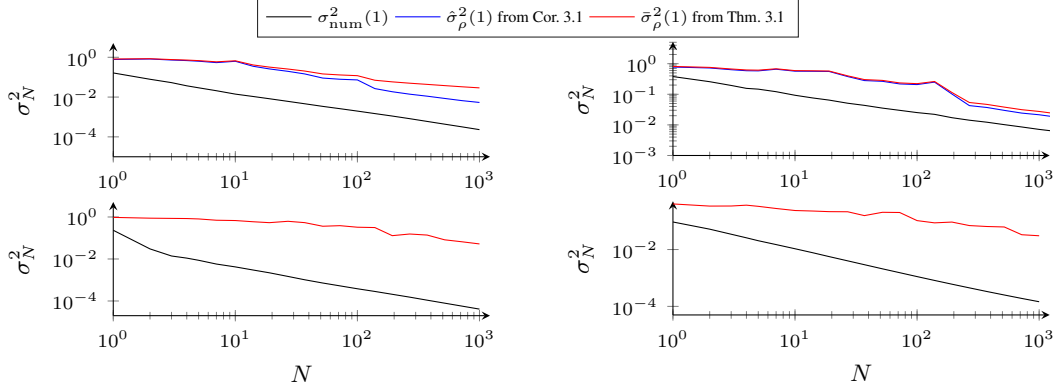


Figure 2: Average posterior variance and bounds of the squared exponential (top left), the Matérn kernel with $\nu = \frac{1}{2}$ (top right), the polynomial kernel with $p = 3$ (bottom left) and the neural network kernel (bottom right) for uniformly sampled training data

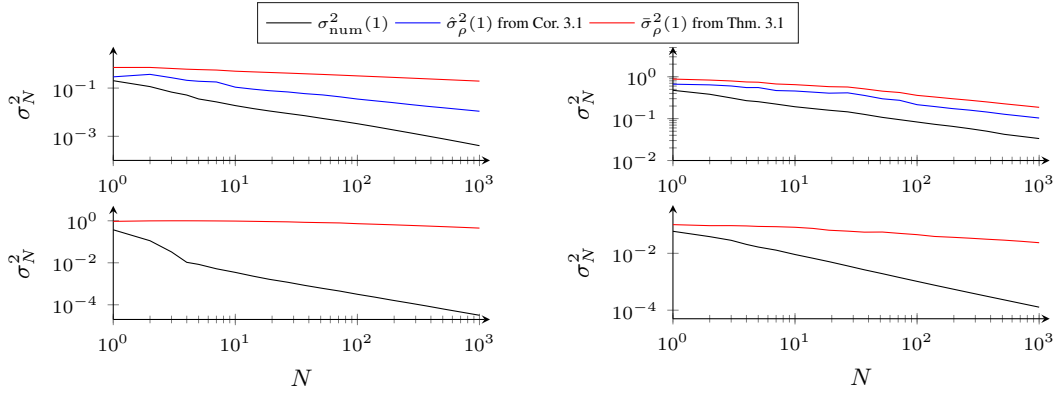


Figure 3: Average posterior variance and bounds of the squared exponential (top left), the Matérn kernel with $\nu = \frac{1}{2}$ (top right), the polynomial kernel with $p = 3$ (bottom left) and the neural network kernel (bottom right) for training data sampled from vanishing distribution

optimal $\rho(N) = cN^{-\frac{1}{2}}$ and $\hat{\sigma}_\rho^2(1) \approx \mathcal{O}(N^{-\frac{1}{2}})$. For these functions $\rho(N)$, the posterior variance bound $\bar{\sigma}_\rho^2(1)$ from Theorem 3.1 and the bound $\hat{\sigma}_\rho^2(1)$ from Corollary 3.1 together with the exact posterior variance $\sigma_{\text{num}}^2(1)$ averaged over 20 different training data sets are illustrated in Fig. 2.

We also compare the bounds in Theorem 3.1 and Corollary 3.1 to the exact posterior variance for training data sampled from the distribution with density function

$$p(x) = 4|1 - x|, \quad 0.5 \leq x \leq 1.5. \quad (21)$$

This probability density vanishes at the test point $x = 1$ and it leads to $\tilde{p}(N) = 4\rho^2(N)$ for $\rho(N) \leq 0.5$. By employing a Taylor expansion of the kernel around the test point, we can derive the optimal asymptotic decay rates for $\rho(N)$ as in the previous section. For the isotropic and the Matérn kernel, this leads to $\rho(N) = cN^{-\frac{1}{3}}$ and an asymptotic behavior of the posterior variance $\sigma_N^2(1) \approx \mathcal{O}(N^{-\frac{1}{3}})$. For the squared exponential kernel, a slightly faster decreasing $\rho(N) = cN^{-\frac{1}{4}}$ can be chosen, which results in $\hat{\sigma}_\rho^2(1) \approx \mathcal{O}(N^{-\frac{1}{2}})$. The curves for the bounds $\bar{\sigma}_\rho^2(1)$ from Theorem 3.1 and $\hat{\sigma}_\rho^2(1)$ from Corollary 3.1 as well as the exact posterior variance averaged over 20 different training data sets for the vanishing training sample distribution are illustrated in Fig. 3.

The posterior variance bounds for the isotropic squared exponential and Matérn kernel exhibit a similar decrease rate as the actually observed one in Fig. 2 and Fig. 3. Indeed, the bound for the Matérn kernel shows the exact same behavior and only differs by a constant factor for large N . However, for non-isotropic kernels, our bound in Theorem 3.1 is rather loose as it converges with $\mathcal{O}(N^{-\frac{1}{2}})$ while the true posterior variance exhibits a decay rate of approximately $\mathcal{O}(N^{-1})$ for the uniform distribution in Fig. 2. Furthermore, no difference of the decrease rate of the numerically estimated posterior variance can be observed between both figures, whereas our bound decreases slightly

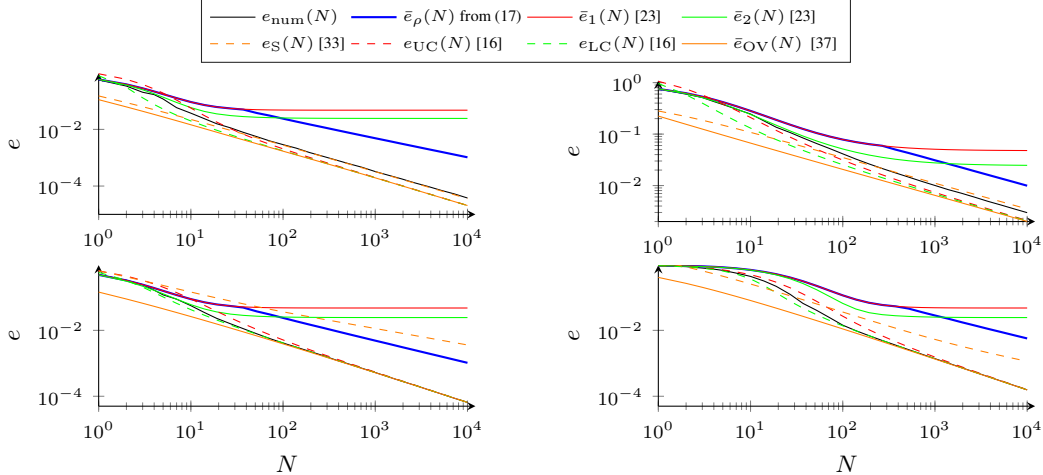


Figure 4: Average learning curve approximations and bounds for the squared exponential (top left), the Matérn kernel (top right), the rational quadratic kernel (bottom left) and the periodic kernel (bottom right); the novel bound (17) converges to zero in contrast to the existing upper bounds from [23]

slower for the vanishing probability distribution in Fig. 3. These two observations are caused by the non-isotropy of these kernels: they consider data globally, while our bound only decreases when training points are added locally around the test point. However, this problem can be overcome by exploiting the special structure of these bounds similarly as in Corollary 3.1, e.g., by using a more suitable distance metric in Theorem 3.1 to define the information radius ρ . Furthermore, the guaranteed decay rate of the variance is already sufficient to ensure that the uniform error bounds in [12, 13] converge to zero for kernels such as, e.g., the linear covariance kernel.

4.2 Average Learning Curves

We pursue a greedy approach to choose n in our learning curve bound (17). We start with $n = 1$ at $N = 1$ and increase n until it reaches a local minimum. For $N > 1$, we start with the value of n from the previous step and perform the same optimization. Note, that the bound (17) is only defined for $n > 1$. Therefore, we make use of (4) for $n = 1$. We compare our learning curve bound (17) to a numerical approximation of the learning curve $e_{\text{num}}(N)$ obtained by averaging over 1000 test points and 50 training data sets for each point in the average learning curve. Furthermore, we evaluate the lower and upper continuous average learning curve approximations $e_{\text{LC}}(N)$ and $e_{\text{UC}}(N)$ [16], respectively, as well as the approximation suggested in [33], which are based on spectral methods. Moreover, we compare our bound to the average learning curve bounds (4) and (6) proposed in [23]. Finally, the lower bound derived in [37] is evaluated. The results of this comparison for the squared exponential, the Matérn, the rational quadratic and the periodic kernel with $l = 0.3$ and noise variance $\sigma_n^2 = 0.05$ are depicted in Fig. 4. Note that σ_n^2 has been subtracted from all curves for illustrative purposes.

Due to the use of (4) in our average learning curve bound for $n = 1$, both curves are identical at the beginning of the plots in Fig. 4. However, for large N our bound outperforms both average learning curve bounds $\bar{e}_1(N)$ and $\bar{e}_2(N)$. In comparison to the average learning curve approximations $e_S(N)$, $e_{\text{UC}}(N)$ and $e_{\text{UL}}(N)$ our average learning curve bound typically differs more strongly from the numerical learning curve $e_{\text{num}}(N)$ as depicted in Fig. 4. However, these are only approximations, hence there is no guarantee that they do not intersect with the true average learning curve. In fact, intersections with $e_{\text{num}}(N)$ can be observed for most of the kernels in Fig. 4. Moreover, it should be noted that the asymptotic behavior of our bound usually does not differ a lot from the true average learning curve. In fact, we can observe the true decay rate of $\mathcal{O}(N^{-\frac{1}{2}})$ for the Matérn kernel [38].

5 Conclusion

In this paper we present a novel bound for the posterior variance of Gaussian processes with Lipschitz continuous kernels. We develop conditions that guarantee its convergence to zero and investigate probability distributions that satisfy these conditions. Furthermore, we demonstrate how the bound can be specialized to smaller classes of kernels and extend it to average learning curve bounds, which can be used for a learning comparison between different kernels.

References

- [1] C. E. Rasmussen and C. K. I. Williams, *Gaussian processes for machine learning*. The MIT Press, 2006.
- [2] F. Berkenkamp, A. Krause, and A. P. Schoellig, “Bayesian Optimization with Safety Constraints: Safe Automatic Parameter Tuning in Robotics,” ETH Zürich, Zürich, Tech. Rep., 2016.
- [3] F. Berkenkamp, A. P. Schoellig, and A. Krause, “Safe Controller Optimization for Quadrotors with Gaussian Processes,” in *Proceedings of the IEEE International Conference on Robotics and Automation*, 2016, pp. 491–496.
- [4] F. Berkenkamp, M. Turchetta, A. P. Schoellig, and A. Krause, “Safe Model-based Reinforcement Learning with Stability Guarantees,” in *Advances in Neural Information Processing Systems*, 2017, pp. 908–918.
- [5] T. Koller, F. Berkenkamp, M. Turchetta, and A. Krause, “Learning-based Model Predictive Control for Safe Exploration and Reinforcement Learning,” in *Proceedings of the IEEE Conference on Decision and Control*, 2018.
- [6] F. Berkenkamp and A. P. Schoellig, “Safe and Robust Learning Control with Gaussian Processes,” in *Proceedings of the European Control Conference*, 2015, pp. 2496–2501.
- [7] J. Umlauf, T. Beckers, M. Kimmel, and S. Hirche, “Feedback Linearization using Gaussian Processes,” in *Proceedings of the IEEE Conference on Decision and Control*, 2017, pp. 5249–5255.
- [8] T. Beckers and S. Hirche, “Gaussian Process based Passivation of a Class of Nonlinear Systems with Unknown Dynamics,” in *Proceedings of the European Control Conference*, 2018.
- [9] J. Umlauf, T. Beckers, and S. Hirche, “Scenario-based Optimal Control for Gaussian Process State Space Models,” in *Proceedings of the European Control Conference*, 2018.
- [10] J. Umlauf, L. Pöhler, and S. Hirche, “An Uncertainty-Based Control Lyapunov Approach for Control-Affine Systems Modeled by Gaussian Process,” *IEEE Control Systems Letters*, vol. 2, no. 3, pp. 483–488, 2018.
- [11] M. K. Helwa, A. Heins, and A. P. Schoellig, “Provably Robust Learning-Based Approach for High-Accuracy Tracking Control of Lagrangian Systems,” in *Proceedings of the IEEE Conference on Decision and Control*, 2018.
- [12] N. Srinivas, A. Krause, S. M. Kakade, and M. W. Seeger, “Information-theoretic regret bounds for Gaussian process optimization in the bandit setting,” *IEEE Transactions on Information Theory*, vol. 58, no. 5, pp. 3250–3265, 2012.
- [13] S. R. Chowdhury and A. Gopalan, “On Kernelized Multi-armed Bandits,” in *Proceedings of the International Conference on Machine Learning*, 2017, pp. 844–853.
- [14] P. Sollich, “Learning Curves for Gaussian Processes,” in *Advances in Neural Information Processing Systems*, 1999, pp. 344–350.
- [15] D. Malzahn and M. Opper, “Learning Curves for Gaussian Processes Regression: A Framework for Good Approximations,” *Advances in Neural Information Processing Systems 13*, pp. 273–279, 2001.
- [16] P. Sollich and A. Halees, “Learning Curves for Gaussian Process Regression: Approximations and Bounds,” *Neural Computation*, vol. 14, pp. 1393–1428, 2002.
- [17] L. Le Gratiet and J. Garnier, “Asymptotic Analysis of the Learning Curve for Gaussian Process Regression,” *Machine Learning*, vol. 98, no. 3, pp. 407–433, 2014.

- [18] Y. Xu, J. Choi, and S. Oh, "Mobile Sensor Network Navigation using Gaussian Processes with Truncated Observations," *IEEE Transactions on Robotics*, vol. 27, no. 6, pp. 1118–1131, 2011.
- [19] E. Schulz, J. B. Tenenbaum, D. N. Reshef, M. Speekenbrink, and S. J. Gershman, "Assessing the Perceived Predictability of Functions," in *Proceedings of the Conference of the Cognitive Science Society*, 2015, pp. 2116–2121.
- [20] T. Ueno, H. Hino, A. Hashimoto, Y. Takeichi, M. Sawada, and K. Ono, "Adaptive Design of an X-ray Magnetic Circular Dichroism Spectroscopy Experiment with Gaussian Process Modeling," *npj Computational Materials*, vol. 4, no. 1, pp. 1–8, 2018.
- [21] D. Reeb, A. Doerr, S. Gerwin, and B. Rakitsch, "Learning Gaussian Processes by Minimizing PAC-Bayesian Generalization Bounds," in *Advances in Neural Information Processing Systems*, 2018.
- [22] A. Krause, A. Singh, and C. Guestrin, "Near-optimal Sensor Placements in Gaussian Processes: Theory, Efficient Algorithms and Empirical Studies," *Journal of Machine Learning Research*, vol. 9, pp. 235–284, 2008.
- [23] C. K. I. Williams and F. Vivarelli, "Upper and Lower Bounds on the Learning Curve for Gaussian Processes," *Machine Learning*, vol. 40, pp. 77–102, 2000.
- [24] F. Vivarelli, "Studies on the Generalisation of Gaussian Processes and Bayesian Neural Networks," Ph.D. dissertation, Aston University, 1998.
- [25] S. Shekhar and T. Javidi, "Gaussian Process Bandits with Adaptive Discretization," *Electronic Journal of Statistics*, vol. 12, pp. 3829–3874, 2018.
- [26] M. L. Stein, *Interpolation of Spatial Data: Some Theory for Kriging*. Springer Science & Business Media, 1999.
- [27] M. Kanagawa, P. Hennig, D. Sejdinovic, and B. K. Sriperumbudur, "Gaussian Processes and Kernel Methods: A Review on Connections and Equivalences," pp. 1–64, 2018. [Online]. Available: <http://arxiv.org/abs/1807.02582>
- [28] Z. M. Wu and R. Schaback, "Local Error Estimates for Radial Basis Function Interpolation of Scattered Data," *IMA Journal of Numerical Analysis*, vol. 13, no. 1, pp. 13–27, 1993.
- [29] H. Wendland, *Scattered Data Approximation*. Cambridge University Press, 2004.
- [30] R. Schaback and H. Wendland, "Kernel Techniques : From Machine Learning to Meshless Methods," *Acta Numerica*, vol. 15, pp. 543–639, 2006.
- [31] R. Beatson, O. Davydov, and J. Levesley, "Error Bounds for Anisotropic RBF Interpolation," *Journal of Approximation Theory*, vol. 162, no. 3, pp. 512–527, 2010.
- [32] M. Scheuerer, R. Schaback, and M. Schlather, "Interpolation of Spatial Data - A Stochastic or a Deterministic Problem ?" *European Journal of Applied Mathematics*, vol. 24, no. 4, pp. 601–629, 2013.
- [33] S. Särkkä and A. Solin, "Continuous-space Gaussian Process Regression and Generalized Wiener Filtering with Application to Learning Curves," in *Image Analysis*, J.-K. Kämäräinen and M. Koskela, Eds. Springer Berlin Heidelberg, 2013, pp. 172–181.
- [34] M. J. Urry and P. Sollich, "Random Walk Kernels and Learning Curves for Gaussian Process Regression on Random Graphs," *Journal of Machine Learning Research*, vol. 14, pp. 1801–1835, 2013.
- [35] K. M. Chai, "Generalization Errors and Learning Curves for Regression with Multi-task Gaussian Processes," *Advances in Neural Information Processing Systems*, pp. 1–9, 2009.
- [36] S. R. F. Ashton and P. Sollich, "Learning Curves for Multi-task Gaussian Process Regression," in *Advances in Neural Information Processing Systems*, 2012, pp. 1393–1428.
- [37] M. Opper and F. Vivarelli, "General Bounds on Bayes Errors for Regression with Gaussian Processes," *Advances in Neural Information Processing Systems*, pp. 302–308, 1999.
- [38] M. Opper, "Regression with Gaussian Processes: Average Case Performance," in *Hong Kong International Workshop on Theoretical Aspects of Neural Computation: A Multidisciplinary Perspective*. World Scientific, 1997, pp. 17–23.
- [39] S. Gershgorin, "Ueber die Abgrenzung der Eigenwerte einer Matrix," *Bulletin de l'Academie des Sciences de l'URSS. Classe des sciences mathematiques et na*, no. 6, pp. 749–754, 1931.

- [40] C. Forbes, M. Evans, N. Hastings, and B. Peacock, *Statistical Distributions*, 4th ed. Hoboken, New Jersey: Wiley, 2011.
- [41] T. H. Cormen, C. E. Leiserson, R. L. Rivest, and C. Stein, *Introduction to Algorithms*, 3rd ed. Cambridge, Massachusetts: The MIT Press, 2009.

A Posterior Variance Bound and Asymptotic Behavior

Proof of Theorem 3.1. Since $\mathbf{K}_N + \sigma_n^2 \mathbf{I}_N$ is a positive definite, quadratic matrix, it follows that

$$\sigma_N^2(\mathbf{x}) \leq k(\mathbf{x}, \mathbf{x}) - \frac{\|\mathbf{k}_N(\mathbf{x})\|^2}{\lambda_{\max}(\mathbf{K}_N) + \sigma_n^2}.$$

Applying the Gershgorin theorem [39] the maximal eigenvalue is bounded by

$$\lambda_{\max}(\mathbf{K}_N) \leq N \max_{\mathbf{x}', \mathbf{x}'' \in \mathbb{D}_N^{\mathbf{x}}} k(\mathbf{x}', \mathbf{x}'').$$

Furthermore, due to the definition of $\mathbf{k}_N(\mathbf{x})$ we have

$$\|\mathbf{k}_N(\mathbf{x})\|^2 \geq N \min_{\mathbf{x}' \in \mathbb{D}_N^{\mathbf{x}}} k^2(\mathbf{x}', \mathbf{x}).$$

Therefore, $\sigma_N^2(\mathbf{x})$ can be bounded by

$$\sigma_N^2(\mathbf{x}) \leq k(\mathbf{x}, \mathbf{x}) - \frac{N \min_{\mathbf{x}' \in \mathbb{D}_N^{\mathbf{x}}} k^2(\mathbf{x}', \mathbf{x})}{N \max_{\mathbf{x}', \mathbf{x}'' \in \mathbb{D}_N^{\mathbf{x}}} k(\mathbf{x}', \mathbf{x}'') + \sigma_n^2}. \quad (22)$$

This bound can be further simplified exploiting the fact that $\sigma_N^2(\mathbf{x}) \leq \sigma_{N-1}^2(\mathbf{x})$ [24] and considering only samples inside the ball $\mathbb{B}_\rho(\mathbf{x})$ with radius $\rho \in \mathbb{R}_+$. Using this reduced data set instead of $\mathbb{D}_N^{\mathbf{x}}$ and writing the right side of (22) as a single fraction results in

$$\sigma_N^2(\mathbf{x}) \leq \frac{k(\mathbf{x}, \mathbf{x})\sigma_n^2 + |\mathbb{B}_\rho(\mathbf{x})| \xi(\mathbf{x}, \rho)}{|\mathbb{B}_\rho(\mathbf{x})| \max_{\mathbf{x}', \mathbf{x}'' \in \mathbb{B}_\rho(\mathbf{x})} k(\mathbf{x}', \mathbf{x}'') + \sigma_n^2}, \quad (23)$$

where

$$\xi(\mathbf{x}, \rho) = k(\mathbf{x}, \mathbf{x}) \max_{\mathbf{x}', \mathbf{x}'' \in \mathbb{B}_\rho(\mathbf{x})} k(\mathbf{x}', \mathbf{x}'') - \min_{\mathbf{x}' \in \mathbb{B}_\rho(\mathbf{x})} k^2(\mathbf{x}', \mathbf{x}).$$

Under the assumption that $\rho \leq \frac{k(\mathbf{x}, \mathbf{x})}{L_k}$ it follows from the Lipschitz continuity of $k(\cdot, \cdot)$ that

$$\min_{\mathbf{x}' \in \mathbb{B}_\rho(\mathbf{x})} k^2(\mathbf{x}', \mathbf{x}) \geq (k(\mathbf{x}, \mathbf{x}) - L_k \rho)^2.$$

Furthermore, it holds that

$$\max_{\mathbf{x}', \mathbf{x}'' \in \mathbb{B}_\rho(\mathbf{x})} k(\mathbf{x}', \mathbf{x}'') \leq k(\mathbf{x}, \mathbf{x}) + 2L_k \rho.$$

Therefore, $\xi(\mathbf{x}, \rho)$ can be bounded by

$$\xi(\mathbf{x}, \rho) \leq 4k(\mathbf{x}, \mathbf{x})L_k \rho - L_k^2 \rho^2.$$

Hence, the result is proven. \square

Proof of Corollary 3.1. The proof follows directly from (23) and the fact that

$$\begin{aligned} \min_{\mathbf{x}' \in \mathbb{B}_\rho(\mathbf{x})} k(\mathbf{x}', \mathbf{x}) &\leq k(\rho) \\ \max_{\mathbf{x}', \mathbf{x}'' \in \mathbb{B}_\rho(\mathbf{x})} k(\mathbf{x}', \mathbf{x}'') &= k(0) \end{aligned}$$

since the kernel is isotropic and decreasing. \square

Proof of Corollary 3.2. The upper bound in Theorem 3.1 converges to zero due to the assumptions on $\rho(N)$ and $|\mathbb{B}_{\rho(N)}(\mathbf{x})|$. Hence, convergence of $\sigma_N^2(\mathbf{x})$ to zero is implied. \square

B Conditions on Probability Distributions for Asymptotic Convergence

In order to prove Theorem 3.2, some auxiliary results for binomial distributions are necessary. These are provided in the following Lemmas.

Lemma B.1. *The k -th central moment of a Bernoulli distributed random variable X is given by*

$$E[(X - E[X])^k] = \sum_{i=0}^{k-1} (-1)^i \binom{k}{i} p^{i+1} + p^k \quad (24)$$

Proof. The polynom $(X - E[X])^k$ can be expanded as

$$(X - E[X])^k = \sum_{i=0}^k \binom{k}{i} (-1)^i X^{k-i} E[X]^i.$$

The k -th moment about the origin of the Bernoulli distribution is given by p for $k > 0$ [40]. Therefore, the expectation of this polynomial is given by

$$E[(X - E[X])^k] = \sum_{i=0}^{k-1} \binom{k}{i} (-1)^i p p^i + p^k,$$

which directly yields the result. \square

Lemma B.2. *The $2k$ -th central moment of a binomial distributed random variable M with $N > 2k$ samples is bounded by*

$$E[(X - E[X])^{2k}] \leq \sum_{m=1}^k (Np)^m \alpha_m \quad (25)$$

where $\alpha_m \in \mathbb{R}$ are finite coefficients.

Proof. A binomial random variable is defined as the sum of N i.i.d. Bernoulli random variables X_i . Therefore, the $2k$ -th central moment of the binomial distribution is given by

$$E[(M - E[M])^{2k}] = E \left[\left(\sum_{i=1}^N (X_i - p) \right)^{2k} \right]. \quad (26)$$

Define the multinomial coefficient as

$$\binom{N}{i_1, i_2, \dots, i_k} = \frac{N!}{\prod_{j=1}^k i_j!}. \quad (27)$$

Then, the sum in the expectation can be expanded, which yields

$$E[(M - E[M])^{2k}] = \sum_{i_1 + i_2 + \dots + i_N = 2k} \binom{2k}{i_1, i_2, \dots, i_N} \prod_{j=1}^N E[(X_j - p)^{i_j}]. \quad (28)$$

This equation expresses the moments of the binomial distribution in terms of the moments of the Bernoulli distribution. Since the first central moment of every distribution equals 0, summands containing a $i_j = 1$ equal 0. Therefore, we obtain the equality

$$E[(M - E[M])^{2k}] = \sum_{\substack{i_1 + i_2 + \dots + i_N = 2k \\ i_j \neq 1 \forall j=1, \dots, N}} \binom{2k}{i_1, i_2, \dots, i_N} \prod_{i_j > 1} E[(X_j - p)^{i_j}]. \quad (29)$$

Moreover, we have

$$E[(X - E[X])^k] = p h_k(p) \quad (30)$$

with

$$h_k(p) = \sum_{i=0}^{k-1} (-1)^i \binom{k}{i} p^i + p^{k-1} \quad (31)$$

due to Lemma B.1. By substituting this into (29) we obtain

$$E[(M - E[M])^{2k}] = \sum_{\substack{i_1 + i_2 + \dots + i_N = 2k \\ i_j \neq 1 \forall j=1, \dots, N}} \binom{2k}{i_1, i_2, \dots, i_N} \prod_{i_j > 1} p h_{i_j}(p). \quad (32)$$

The product can have between 1 and k factors due to the structure of the problem. Therefore, it is not necessary for the sum to consider all N coefficients i_j , but rather consider only $1 \leq m \leq k$ coefficients which are greater than 1. This leads to the following equality

$$E[(M - E[M])^{2k}] = \sum_{m=1}^k \binom{N}{m} p^m \sum_{\substack{i_1 + i_2 + \dots + i_m = 2k \\ i_j > 1 \forall j=1, \dots, m}} \binom{2k}{i_1, i_2, \dots, i_m} \prod_{i_j > 1} h_{i_j}(p). \quad (33)$$

Due to [41] it holds that $\binom{N}{m} \leq \frac{N^m}{m!}$. Furthermore, the functions $h_k(\cdot)$ can be upper bounded by $\sum_{i=1}^k \binom{k}{i} = 2^k$ because $0 \leq p \leq 1$. Therefore, we can upper bound the $2k$ -th central moment of the binomial distribution by

$$E[(M - E[M])^{2k}] \leq \sum_{m=1}^k (Np)^m \alpha_m \quad (34)$$

with

$$\alpha_m = \frac{\sum_{\substack{i_1+i_2+\dots+i_m=2k \\ i_j > 1 \forall j=1,\dots,m}} \binom{2k}{i_1, i_2, \dots, i_m} \prod_{i_j > 1} 2^{i_j}}{m!} \quad (35)$$

and the result is proven. \square

The restriction to $N > 2k$ samples allows to derive a relatively simple expression for the expansion in (28). However, the bound (25) also holds without this condition, since it only guarantees that for $i_j = 1, \forall j = 1, \dots, N, \sum_{j=1}^N i_j \geq 2k$ and therefore, all possible combinations of i_j can be estimated simpler in (33). Hence, the corresponding summands in (35) can be considered 0 for $N \leq 2k$ and the upper bound (25) still holds for $N \leq 2k$.

Proof of Theorem 3.2. We have to show that the number of samples from the probability distribution with density $p(\cdot)$ inside the balls with radius $\rho(N)$ grows to infinity for $N \rightarrow \infty$. The number of samples $|\mathbb{B}_{\rho(N)}(\mathbf{x})|$ follows a binomial distribution with mean

$$E[|\mathbb{B}_{\rho(N)}(\mathbf{x})|] = N\tilde{p}(N),$$

where

$$\tilde{p}(N) = \int_{\{\mathbf{x}' \in \mathbb{X}: \|\mathbf{x} - \mathbf{x}'\| \leq \rho(N)\}} p(\mathbf{x}') d\mathbf{x}'$$

is the probability of a sample lying inside the ball around \mathbf{x} with radius $\rho(N)$ for fixed $N \in \mathbb{N}$. Since we have

$$\int_{\{\mathbf{x}' \in \mathbb{X}: \|\mathbf{x} - \mathbf{x}'\| \leq \rho(N)\}} p(\mathbf{x}') d\mathbf{x}' \geq cN^{-1+\epsilon} \quad (36)$$

by assumption, this mean goes to infinity, i.e.

$$\lim_{N \rightarrow \infty} E[|\mathbb{B}_{\rho(N)}(\mathbf{x})|] = \lim_{N \rightarrow \infty} cN^\epsilon = \infty.$$

Therefore, it is sufficient to show that $|\mathbb{B}_{\rho(N)}(\mathbf{x})|$ converges to its expectation almost surely, which is identically to proving that

$$\lim_{N \rightarrow \infty} \frac{|\mathbb{B}_{\rho(N)}(\mathbf{x})|}{E[|\mathbb{B}_{\rho(N)}(\mathbf{x})|]} = 1 \quad a.s.$$

Due to the Borel-Cantelli lemma, this convergence is guaranteed if

$$\sum_{N=1}^{\infty} P\left(\left|\frac{|\mathbb{B}_{\rho(N)}(\mathbf{x})|}{E[|\mathbb{B}_{\rho(N)}(\mathbf{x})|]} - 1\right| > \xi\right) < \infty \quad (37)$$

holds for all $\xi > 0$. The probability for each $N \in \mathbb{N}$ can be bounded by

$$P\left(\left|\frac{|\mathbb{B}_{\rho(N)}(\mathbf{x})|}{N\tilde{p}(N)} - 1\right| > \xi\right) \leq \frac{E\left[\left(|\mathbb{B}_{\rho(N)}(\mathbf{x})| - N\tilde{p}(N)\right)^{2k}\right]}{(\xi N\tilde{p}(N))^{2k}}.$$

for each $k \in \mathbb{N}_+$ due to Chebyshev's inequality, where the $2k$ -th central moment of the binomial distribution can be bounded by

$$E\left[\left(|\mathbb{B}_{\rho(N)}(\mathbf{x})| - N\tilde{p}(N)\right)^{2k}\right] \leq \sum_{i=1}^k \alpha_i \tilde{p}^i(N) N^i$$

with some coefficients $\alpha_i < \infty$ due to Lemma B.2. Therefore, we can bound each probability in (37) by

$$P\left(\left|\frac{|\mathbb{B}_{\rho(N)}(\mathbf{x})|}{N\tilde{p}(N)} - 1\right| > \xi\right) \leq \sum_{i=1}^k \alpha_i \tilde{p}^{-2k+i}(N) N^{-2k+i}.$$

Due to (36) this bound can be simplified to

$$P\left(\left|\frac{|\mathbb{B}_{\rho(N)}(\mathbf{x})|}{N\tilde{p}(N)} - 1\right| > \xi\right) \leq N^{-k\epsilon} \sum_{i=0}^{k-1} \tilde{\alpha}_{k-i} N^{-i\epsilon},$$

where $\tilde{\alpha}_i = c^{-2k+i} \alpha_i$. Let $k = \lceil \frac{1}{\epsilon} \rceil + 1$. Then, each exponent is smaller than or equal to $-1 - \epsilon$. Hence, the sum of probabilities can be bounded by

$$\sum_{N=1}^{\infty} P\left(\left|\frac{|\mathbb{B}_{\rho(N)}(\mathbf{x})|}{N\tilde{p}(N)} - 1\right| > \xi\right) \leq \sum_{i=0}^{k-1} \tilde{\alpha}_{k-i} \zeta((k+i)\epsilon),$$

where $\zeta(\cdot)$ is the Riemann zeta function, which has finite values. Therefore, we obtain

$$\sum_{N=1}^{\infty} P\left(\left|\frac{|\mathbb{B}_{\rho(N)}(\mathbf{x})|}{N\tilde{p}(N)} - 1\right| > \epsilon\right) < \infty$$

and consequently, the theorem is proven. \square

Proof of Corollary 3.3. Let

$$\begin{aligned} \bar{p} &= \min_{\|\mathbf{x}-\mathbf{x}'\| \leq \xi} p(\mathbf{x}') \\ \tilde{p}(N) &= \int_{\{\mathbf{x}' \in \mathbb{X}: \|\mathbf{x}-\mathbf{x}'\| \leq \xi\}} p(\mathbf{x}') d\mathbf{x}', \end{aligned}$$

where \bar{p} is positive by assumption. Then, we can bound $\tilde{p}(N)$ by

$$\tilde{p}(N) \geq \bar{p} V_d \rho^d(N),$$

where V_d is the volume of the d dimensional unit ball. Since $\rho(N) \geq cN^{-\frac{1}{d}+\epsilon}$ for some $c, \epsilon > 0$ by assumption, it follows that

$$\tilde{p}(N) \geq \bar{p} V_d c N^{-1+\frac{\epsilon}{d}}.$$

Hence, $\tilde{p}(N)$ satisfies the conditions of Theorem 3.2, which proves the corollary. \square